Inferring ultraviolet anatomical exposure patterns while distinguishing the relative contribution of radiation components

Laurent Vuilleumier, Antoine Milon, Jean-Luc Bulliard, Laurent Moccozet, and David Vernez

Citation: AIP Conf. Proc. **1531**, 792 (2013); doi: 10.1063/1.4804889
View online: http://dx.doi.org/10.1063/1.4804889
View Table of Contents: http://proceedings.aip.org/dbt/dbt.jsp?KEY=APCPCS&Volume=1531&Issue=1
Published by the American Institute of Physics.

Inferring Ultraviolet Anatomical Exposure Patterns while Distinguishing the Relative Contribution of Radiation Components

Laurent Vuilleumier[a], Antoine Milon[b], Jean-Luc Bulliard[c], Laurent Moccozet[d] and David Vernez[b]

[a]*Federal Office of Meteorology and Climatology, MeteoSwiss, Payerne, Switzerland*
[b]*Institute of Work and Health, University of Lausanne and Geneva, Lausanne, Switzerland*
[c]*Cancer Epidemiology Unit, Centre Hospitalier Universitaire Vaudois and University of Lausanne, Lausanne, Switzerland*
[d]*Institute of Services Science, University of Geneva, Switzerland*

Abstract. Exposure to solar ultraviolet (UV) radiation is the main causative factor for skin cancer. UV exposure depends on environmental and individual factors, but individual exposure data remain scarce. While ground UV irradiance is monitored via different techniques, it is difficult to translate such observations into human UV exposure or dose because of confounding factors. A multi-disciplinary collaboration developed a model predicting the dose and distribution of UV exposure on the basis of ground irradiation and morphological data. Standard 3D computer graphics techniques were adapted to develop a simulation tool that estimates solar exposure of a virtual manikin depicted as a triangle mesh surface. The amount of solar energy received by various body locations is computed for direct, diffuse and reflected radiation separately. Dosimetric measurements obtained in field conditions were used to assess the model performance. The model predicted exposure to solar UV adequately with a symmetric mean absolute percentage error of 13% and half of the predictions within 17% range of the measurements.

Using this tool, solar UV exposure patterns were investigated with respect to the relative contribution of the direct, diffuse and reflected radiation. Exposure doses for various body parts and exposure scenarios of a standing individual were assessed using erythemally-weighted UV ground irradiance data measured in 2009 at Payerne, Switzerland as input. For most anatomical sites, mean daily doses were high (typically 6.2-14.6 Standard Erythemal Dose, SED) and exceeded recommended exposure values. Direct exposure was important during specific periods (e.g. midday during summer), but contributed moderately to the annual dose, ranging from 15 to 24% for vertical and horizontal body parts, respectively. Diffuse irradiation explained about 80% of the cumulative annual exposure dose.

INTRODUCTION

Solar ultraviolet (UV) radiation is one of few environmental exposures that can both cause and protect against diseases. While UV exposure can prevent diseases of vitamin D insufficiency, it can cause eye diseases and is responsible for 50–90% of all skin cancers [1]. Each year, excessive sun exposure leads to about 60 000 premature skin cancer deaths worldwide, the majority of these being melanomas [2]. Although epithelial skin cancer is less lethal than melanoma, it is the most common cancer among fair-skinned people with an annual burden of approximately 10 million basal cell carcinomas (BCCs) and 2.9 million squamous cell carcinomas (SCCs) [2]. The dose-response between UV exposure patterns and skin cancer occurrence is not yet fully understood. SCC is primarily induced by chronic (cumulative) sun exposure, leaving outdoor workers and elderly people at greater risk [3,4]. Melanoma has been associated with intermittent sun exposure [5], while both cumulative exposure and intermittent exposure appear to be responsible for BCC development [6]. For a given individual, the anatomical distribution of UV exposure is highly heterogeneous, poorly correlated to ground irradiance, and depends on the time of exposure and orientation to the sun [7]. Variations in UV doses received across individuals are even greater as they are strongly influenced by behavioral and host factors such as posture, orientation to the sun, skin complexion, clothing and other sun-protective behaviors [8,9]. UV protection messages often focus on direct radiation and short-term, acute exposure (avoidance of erythema), implicitly assuming that direct UV radiation is the key contributor to the overall UV exposure. However, little is known regarding the relative contribution of the direct, diffuse and reflected UV radiation to the anatomical exposure as individual dosimetric measurement cannot separate the three radiation components. Recent investigations of UV doses received by body parts shielded from direct sunlight have suggested the importance of diffuse radiation [10,11].

Radiation Processes in the Atmosphere and Ocean (IRS2012)
AIP Conf. Proc. 1531, 792-796 (2013); doi: 10.1063/1.4804889

THE SIMUVEX UV EXPOSURE SIMULATION TOOL

Our model, *Simulating UV Exposure* (SimUVEx) [12], uses continuous datasets of erythemally-weighted UV ground irradiance to estimate the dose and anatomical distribution of UV received by exposed individuals (Fig. 1). The data are fed into a ray-tracing algorithm in which direct $I(t)$, diffuse $D(t)$ and reflected $R(t)$ (reflection from ground) components are separately taken into account. Exposure to various anatomical locations is obtained by exposing a 3D virtual manikin to a local radiation sphere, discretized into n sub-surfaces, for a given duration. The exposure levels and doses computed during the simulation can be visualized as comprehensive 3D images using expressive rendering techniques.

Three ambient irradiance time series are required as input parameters to the model for the direct, the diffuse and the ground reflected irradiance (W/m^2), as well as the sun position, defined by its azimuth $p(t)$ and zenith $d(t)$ angles. The model derives radiances distributed on a local sphere from these inputs using simplifying hypotheses. Such input data can be obtained from meteorological stations equipped with multiple broadband radiometers (e.g. one for direct, one for diffuse radiation with a shadowing disc and one turned upside down for reflected radiation). Alternatively these data can be obtained from atmospheric radiation transfer models (RTM). In clear-sky situations, RTM give accurate estimates of the irradiance components, but their use is more questionable in cloudy situations. For complex cloudy situations, efforts are currently devoted to reconstructing UV irradiance based on proxies.

Deriving UV exposure from irradiance is based on simplifying the reflected $R(t)$ and diffuse $D(t)$ components as hemispherical quasi-isotropic sources (azimuthal isotropy, and limited zenith dependence) with time-dependent intensities (Fig. 1, center). The direct component $I(t)$ is described as a parallel source of radiation varying in intensity with time and in direction with the sun position.

Traditional 3D human modeling and animation approaches, based on articulated skeleton and 3D surface skinning [13] are used to produce a 3D virtual manikin with variable morphologies in standard working positions. Postures are defined as a set of angles values defined at joint articulations of a simplified skeleton. Its surface is depicted as a single 3D mesh of connected triangles, whose density depends on the desired resolution (here optimizing computing time and level of body detail results in ~4000 triangles). Manikin models are produced with the open source software MakeHuman [14]. Each triangle of the manikin receives a specific amount of radiation according to its exposure to the different virtual sources of radiation. This is the average of the exposures computed at the vertices, which are functions of radiation intensity, orientations of triangles and light sources as well as shading from body parts (Fig. 2).

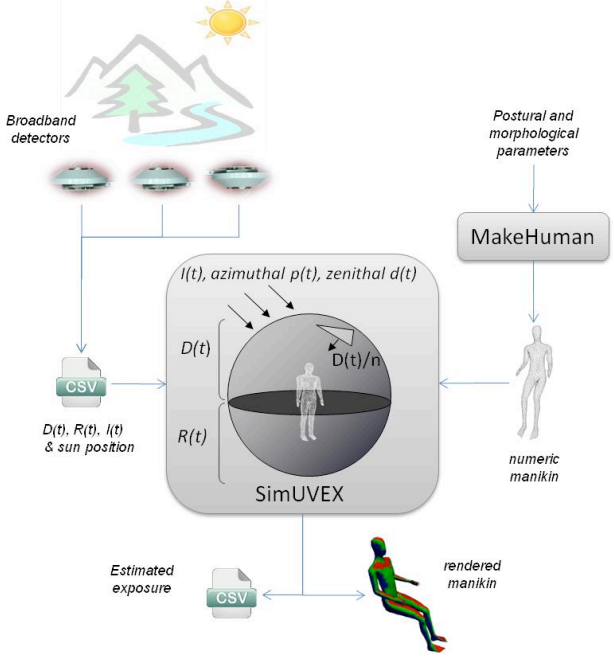

FIGURE 1. Schematic view of the SimUVEx model.

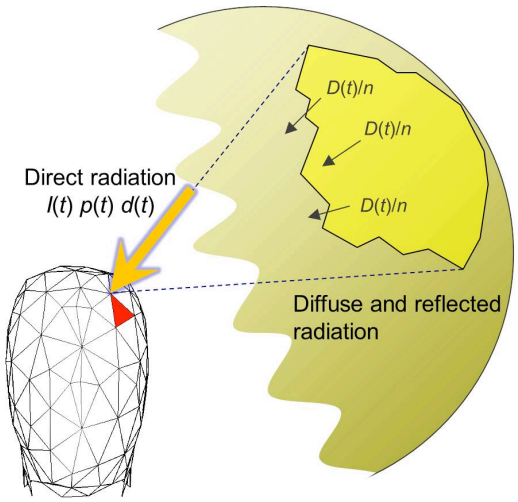

FIGURE 2. Computation of energy received at a vertex.

DATA

Measurements performed at the MeteoSwiss Payerne station (46.815°N, 6.944°E, altitude 491 m) were used. This station belongs to the Baseline Surface Radiation Network of the World Meteorological Organization. Direct, diffuse and reflected UV irradiance are measured concomitantly every minute at this facility using broadband UV radiometers (SolarLight biometer 501A) with filters mimicking the erythemal response [15]. Instruments measuring direct and diffuse components are mounted on sun-trackers (within a collimator for direct and under a shading disc for diffuse), while the one measuring the reflected component is turned upside down. These broadband radiometers undergo strict quality assurance procedures including regular calibrations traceable to the European Ultraviolet Calibration Centre [16]. The calibration technique accounts for differences between the spectral response of the filter and the theoretical erythemal action spectrum. The overall uncertainty of the measurement is estimated at 10%.

Model validation field measurements were collected in May and June 2007. For validation, we used dosimetric measurements made with CIE erythemally weighted Spore film dosimeters (Bio-Sense, Bornheim, Germany) positioned on an articulated foam manikin as individual exposure measurements. The dosimeters lower detection limit was 100 J/m^2 (1 SED) with accuracy ranging from 5 to 20% (standard deviation, SD) for laboratory and unfavorable field conditions, respectively [17,18]. We used a SD of 15% for our field conditions. We investigated 5 static postures: seated, kneeling, standing bowing, standing erect arms down, and standing erect arms up, and investigated 8 body locations: neck, lower back, left and right shoulders, right wrist, chest, forehead, and top head. In total, 54 dosimeters were used.

UV irradiance data collected during the entire year 2009 were used in a further study of outdoor worker exposure [19]. These data were first screened for missing or aberrant values (e.g. maintenance of the measuring device) resulting in less than 0.5% of the sample being rejected. These missing or aberrant values (except 35 minute data) were recalculated using ground global UV irradiance.

SIMUVEX VALIDATION

The field validation results for various body postures and body locations are presented in Fig. 3. SimUVEx predictions were on the same order of magnitude as the measured values and agreed overall with the expected values (gray line). The symmetric mean absolute percentage error (sMAPE) was 13%. Half of the predictions fell within a 17% range of the measurements and 75% within a 40% range of the measurements.

Several main uncertainty sources can explain the differences observed between predicted and measured values: the field measurement procedure, accuracy of the spore film dosimeters, and the model hypothesis. It was difficult to have an exact match between the posture and morphology of the foam and virtual manikins. This may lead to discrepancies in both orientation and shading of the body surfaces. Moreover, due to their shape and size, dosimeters may have a slightly different orientation compared to body surfaces. Such uncertainties are not accounted for in the 15% dosimetric error, but may contribute significantly to the overall uncertainty. Uncertainties also arise from the model radiance derived from irradiance measurements. Careful and regular calibrations were made for reducing the irradiance uncertainty, which is on the order of 10% for 1 min data. Part of it is statistical variation and is reduced with longer aggregation times, but a 5–8% uncertainty remains from calibration procedures alone.

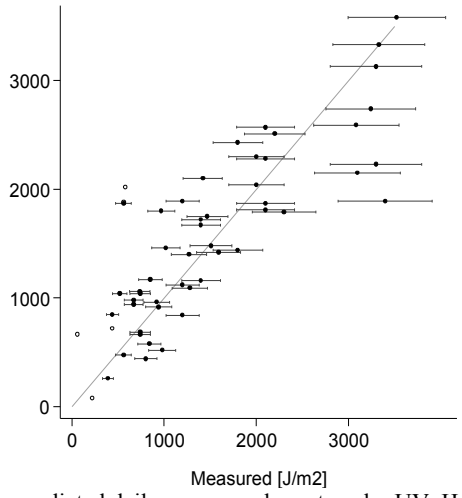

FIGURE 3. Measured *vs.* predicted daily exposure doses to solar UV. Hollow dots are excluded outliers.

STUDY OF UV EXPOSURE FOR OUTDOOR WORKERS

Over 2009, high mean daily doses, between 6.2 and 14.6 standard erythemal doses (SED, 100 J/m^2) were obtained, which exceeded both the International Commission on Non-ionizing Radiation Protection exposure threshold (0.3 SED [20]) and minimal erythema dose for skin types II and III (2.5‑ 3.0 SED [21]) the most common phototypes in fair-skinned populations. These daily doses assumed unprotected skin and year-round exposure so that results represent upper dose estimates. Horizontal body parts, such as top of shoulder, exhibited highest exposure doses. For most anatomical sites, exposure was ~half the ambient horizontal total dose. The strongest attenuation was observed for vertical and curved body sections such as the back of the hand (6.2 SED) or the face (6.7 SED) that were exposed to 38% and 41% of the ambient total dose (16.3 SED), respectively.

Reflected radiation bore a negligible contribution (except on winter days with snow cover) and most UV exposure was from diffuse & direct irradiation. Significant direct irradiation contribution occurred only for specific times and body locations: representing up to 50% of top of shoulder dose for some summer days around midday. But direct irradiation exposure was strongly attenuated by shading from other body parts, lower sun zenith angle (daily/seasonal cycles), and cloudiness, explaining low overall contribution of direct irradiation to yearly cumulative dose: 24% for horiz. surfaces, and less for vert. & curved body parts (19% for neck & shoulders and 15% for face).

Diffuse irradiation was responsible for ~80% of the yearly exposure dose, and was main contributor to average exposure. It exhibited only limited anatomical variations, ranging from 76% for top of shoulder to 82% for vert. or curved body parts (face, center back, forearm, legs). Fig. 4 shows daily exposure doses and relative contribution from each type of irradiation for face, neck & top of shoulder. These sites were of special interest because they are often uncovered, have various orientations and have been associated with BCC and SCC (at least for face and neck).

Differences in seasonal patterns of exposure across body parts are apparent on Fig. 4. Both the direct and diffuse irradiation exhibited a marked yearly cycle, the former being stronger than the latter. The increase in daily dose for neck and top of shoulder during summer led to daily exposures up to 40 SED. This strong yearly cycle is due to seasonal change in solar zenith angle. In addition, clouds are frequent at Payerne, which impacts most on direct radiation. On average, the neck was 31% less exposed than the top of shoulder on cloudy winter days. The decrease in direct exposure for vertical body parts explains why facial exposure was lower than both neck and top of shoulder exposure. Interestingly, diffuse exposure was also 50% lower for the face compared with top of shoulder. This decrease is due to the fact that vertical body parts are exposed to a smaller part of the sky than horizontal ones.

Further investigations were performed for specific days to better understand exposure patterns and their influencing factors. Vernez et al. [19] present more details on these specific investigations contrasting the component contributions on clear-sky and cloudy days for the various seasons.

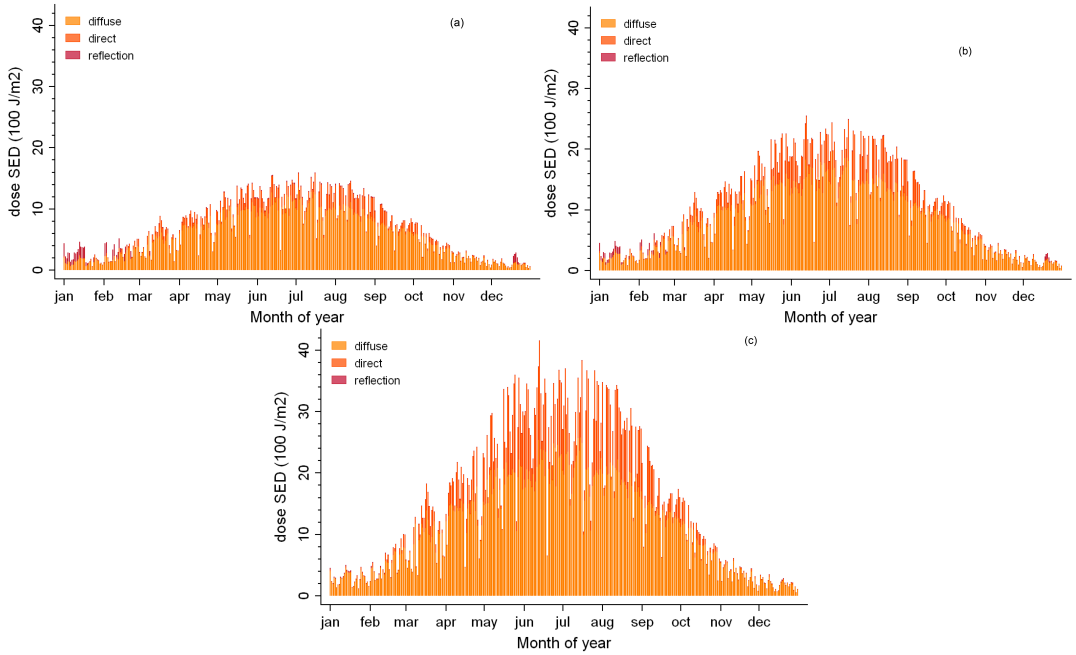

FIGURE 4. UV daily doses (2009) at Payerne for adult man standing, arms down, (a, top left) face, (b, top right) neck, and (c, bottom left) top of shoulder.

DISCUSSION

As any model, SimUVEx has limitations due to underlying simplifying hypotheses [12]. First, diffuse&reflected radiation were assumed to be near isotropic, but the clear-sky diffuse component is expected to be anisotropic. Second, the model simulated year-round exposure of unprotected skin. This overestimated real exposure, but provided an upper annual potential exposure, leaving room to predict attenuating effects of sun-protection scenarios. It does also not affect relative comparisons. Third, results pertain to a standing posture (arms down). Although this predominates for outdoor construct. workers, activities characterized by other postures may differ in site-specific UV exposure. Our estimates of global anatomical UV exp. (sum of all components) were in line with studies based on rotating manikins & living subjects. Proportion of ground irradiance received by the face (about 41% in our study), hand dorsum (38%) and calf (44%) agreed with manikin-based measures [22,23]. Our predicted exposure patterns agreed with dosimetric measurements on agricult. workers in Denmark [24] & Italy [25]. Studies of similar designs exhibited discrepancies for given anatomical: dosimetric assessment of manikin shoulder exposure was 85-90% of value at head vertex accord. to Wright et al. [22] and 66-75% accord. to Diffey [23]. SimUVEx yielded an ambient exposure ratio of 57% (whole shoulder) & 90% (top of shoulder) illustrating effect of assessment technique. Dosimetry only captures a single local exposure; our model can also average dose over whole areas and explains apparently conflicting results. Our results suggest a predominant contribution of diffuse UV radiation to total sun exposure. Predicted situations of high direct radiation typic. corresponded to situations of potential acute over-exposure episodes. Such high-risk situations are usually covered in sun-protection messages. But the importance of diffuse radiation, albeit the main contributor to total UV exposure, doesn't appear to be adequately conveyed in current prevention messages. Our results question effectiveness of current recommendations regarding subsequent risk of long-term UV damage, such as non-melanocytic lesions. It is particularly true for vert. oriented surfaces such as the face, for which diffuse exposure explained most of the yearly dose, or for cloudy summer days where UV radiation stays high and is much higher than on sunny days in other seasons. Sun-protection messages tailored towards chronically exposed outdoor workers could include long-term risk associated with a regular exposure to suberythemal UV doses, and information about the limited protection offered by clouds (especially in summer).

REFERENCES

1. WHO, Solar and Ultraviolet Radiation. IARC monographs on the evaluation of carcinogenic risks to humans, London: World Health Organization, 1992.
2. R. M. Lucas, A. J. McMichael, B. K. Armstrong and W. T. Smith, *Int. J. Epidemiol.* **37**:13, 654–667 (2008).
3. B. K. Armstrong and A. Kricker, *J. Photochem. Photobiol. B* **63**, 8–18 (2001).
4. J. Schmitt, A. Seidler, T. L. Diepgen and A. Bauer, *Br. J. Dermatol.* **164**, 291–307 (2011).
5. J. M. Elwood and J. Jopson, *Int. J. Cancer* **73**, 198–203 (1997).
6. A. Bauer, T. L. Diepgen and J. Schmitt, *Br. J. Dermatol.* **165**, 612–625 (2011).
7. A. V. Parisi, M. G. Kimlin, J. C. F. Wong and R. A. Fleming, *Photodermatol. Photoimmunol. Photomed.* **12**, 66–72 (1996).
8. P. Autier, M. Boniol and J.-F. Doré, *Int J Cancer* **121**, 1–5 (2007).
9. A. V. Parisi, M. G. Kimlin, R. Lester and D. Turnbull, *J. Photochem. Photobiol. B* **69**, 1–6, 2003.
10. D. J. Turnbull and A. V. Parisi, *J. Photochem. Photobiol. B* **69**, 13–19 (2003).
11. M. G. Kimlin, N. Martinez, A. C. Green and D. C. Whiteman, *J. Photochem. Photobiol. B* **85**, 23–27 (2006).
12. D. Vernez et al., *Photochem. Photobiol.* **87**:13, 721–728 (2011).
13. T. Di Giacomo, H. Kim, L. Moccozet and N. Magnenat-Thalmann, Control structure and multi-resolution techniques for virtual human representation, in *Shape Analysis and Structuring*, Berlin, Springer Verlag, 2007, 245–268.
14. MakeHuman, Open source tool for making 3D characters. Avail. on-line: http://www.makehuman.org/ (2012).
15. A. F. McKinlay and B. L. Diffey, A reference action spectrum for ultra-violet induced erythema in human skin, in *Human Exposure to Ultraviolet Radiation: Risks and Regulations*, Amsterdam, Elsevier Science Ltd, 1987, 83–87.
16. G. Hülsen and J. Gröbner, *Appl. Opt.* **46**, 5877–5886 (2007).
17. M. Moehrle, M. Korn and C. Garbe, *Int. Arch. Occup. Environ. Health* **73**, 575–580 (2000).
18. Y. Furusawa, L. E. Quintern, H. Holtschmidt, K. P and M. Saito, *Appl. Microbiol. Biotechnol.* **50**, 597–603 (1998).
19. D. Vernez, A. Milon, L. Vuilleumier and J.-L. Bulliard, *Br. J. Dermatol.* **167**:12, 383–390 (2012).
20. International Commission on Non-ionizing Radiation Protection (ICNIRP), *Health Phys.* **87**, 171–186 (2004).
21. S. Dornelles, J. Goldim and T. Cestarl, *Photochem. Photobiol.* **79**, 540–544 (2004).
22. C. Wright, R. Diab and B. Martincigh, *S. Afr. J. Sci.* **100**, 498–500 (2004).
23. B. L. Diffey, *Phys. Med. Biol.* **36**, 299–328 (1991).
24. E. Thieden, P. A. Philipsen, J. Heydenreich and H. C. Wulf, *Arch. Dermatol.* **140**:12, 197–203 (2004).
25. A. M. Siani et al., *Photochem. Photobiol.* **87**, 925–934 (2011).